frontiers | Frontiers in Energy Research

TYPE Methods
PUBLISHED 22 April 2024
DOI 10.3389/fenrg.2024.1369452

OPEN ACCESS

EDITED BY
Kaiping Qu,
China University of Mining and Technology, China

REVIEWED BY
Da Xu,
China University of Geosciences Wuhan, China
Feifan Shen,
Hunan University, China

*CORRESPONDENCE
Fuju Zhou,
fujuzhou_sg@sina.com

RECEIVED 12 January 2024
ACCEPTED 19 February 2024
PUBLISHED 22 April 2024

CITATION
Zhou F, Zhou P, Shi T, Jing J, Liang G, Xu S, Zhou J and Yang K (2024), Resilience-oriented repair crew and network reconfiguration coordinated operational scheduling for post-event restoration.
Front. Energy Res. 12:1369452.
doi: 10.3389/fenrg.2024.1369452

Resilience-oriented repair crew and network reconfiguration coordinated operational scheduling for post-event restoration

Fuju Zhou[1]*, Peng Zhou[2], Tianchen Shi[3], Jiangping Jing[4], Gaige Liang[2], Shengrong Xu[1], Jianda Zhou[1] and Kai Yang[1]

[1]State Grid Suqian Power Supply Company, Suqian, China, [2]State Grid Xuzhou Power Supply Company, Xuzhou, China, [3]College of Energy and Electrical Engineering, Hohai University, Nanjing, China, [4]State Grid Jiangsu Electric Power Co., Ltd., Nanjing, China

This paper introduces a post-disaster load restoration approach for the distribution grid, utilizing network reconfiguration (NR) and dispatching of repair crews (RCs) to significantly enhance grid resilience. We propose an RC–NR coordinated model that leverages diverse flexible resources within the active distribution network (ADN), aimed at not only enhancing the grid's resilience level but also efficiently mending the fault lines. The model introduces fault repairing and sequential NR coupled constraints to devise an optimal resilience strategy within temporal domain cooperation, focusing on minimizing repair and penalty costs associated with the restoration process. To tackle the challenge of computational complexity, the nonlinear model is reformulated into a mixed-integer second-order cone programming model. The efficacy of the approach is validated through case studies on an IEEE 33-bus system, in which simulation results demonstrate a considerable improvement in grid resilience, achieving optimal load recovery with reduced restoration time and costs. The proposed approach outperforms traditional methods with optimal repair sequence and RC scheduling, aligned with NR efforts, and contributes to an improved system resilience level.

KEYWORDS

resilience, active distribution network, repair crews, restoration, load recovery

1 Introduction

In recent decades, a series of frequent and severe extreme events, exemplified by incidents like the 2021 Texas power blackouts (Zhang et al., 2022), the Zhengzhou flood blackouts, and the Taiwan rolling blackouts in 2022, have had a profound impact on grid resilience (Perera et al., 2020). These occurrences have resulted in energy deficiencies and prolonged power interruptions, posing a severe challenge to the power system operation. Concurrently, the power distribution network is undergoing a significant transition from the traditional network to the active distribution network (ADN). Explicitly highlighted during the 2008 International Large Power Grid Conference, the ADN possesses the capability to autonomously control and manage locally distributed energy resources (DERs), adjusting the network topology in real time based on the system operational

status to precisely regulate the power flow (Li et al., 2017). This concept has been consistently embraced within the academic community. It is crucial to emphasize that unlike the autonomy of microgrids, under normal circumstances, the ADN, as a public distribution network managed by power companies, does not permit islanded operation. However, in emergency situations, a judicious configuration of switching points can enable specific areas of the ADN to function as isolated microgrids in an unconventional manner to support the ADN operation (Konakalla et al., 2019). Therefore, leveraging the resources within the ADN to enhance its resilience against extreme natural disasters is of paramount significance, aiming to mitigate economic losses caused by power outages.

As the foundation for the resilience operation of the ADN, it is crucial to model and evaluate the fault scenarios caused by extreme disasters. Typhoons are one of the most frequently occurring extreme disasters. Mu et al. (2022), using the classic Batts typhoon model, obtained time-varying wind speed curves at various points of the lines. Combining the vulnerability model of distribution network components, they generated fault scenarios using a non-time-series Monte Carlo simulation method. Hussain et al. (2019) considered the spatial distribution characteristics of faulty and outage equipment under typhoon disasters, categorizing them into centralized, decentralized, and centralized–decentralized distributions. They generated a set of fault scenarios for the ADN based on the fault rate distribution functions of different typhoon grades. Hou et al. (2021), starting from historical data on typhoon damage, established a prediction and evaluation model for user power outage grids under typhoon disasters using data mining and grid partitioning methods. Building upon classical models, Hou et al. (2023) made uncertainty improvements to the typhoon wind field and line fault models, considering the effects of diverse wind speeds. They proposed an improved model for line stress interference. In summary, the existing models describe the time and space characteristics of typhoons, analyze the impact mechanism of extreme disasters on distribution networks, and ultimately determine damaged scenarios by establishing component vulnerability models. These above research studies provide the fundamental models and methods for evaluating the potential faults of extreme disasters, which contributes to further investigation of the resilience operation methods.

To deal with the extreme disasters, the main measures adopted include network reconfiguration (NR) and emergency islanding. The ADNs are generally designed as closed-loop systems but operate in an open-loop manner to improve the reliability of the system. This characteristic provides a prerequisite for the implementation of network reconstruction and islanding. The NR involves the rational configuration of tie points, remotely activating or deactivating the corresponding circuit breakers, allowing specific local areas of the distribution network to operate as microgrids in an abnormal state. By this measure, the critical loads can be supplied to avoid economic losses. Demetriou et al. (2016) and Liu et al. (2019a) formulated the islanding division and power output adjustment problem as a mixed-integer linear programming model. They determined optimal islanding strategies by first obtaining a DC-feasible solution and then determining the operating point for AC steady-state islanding. Hafez et al. (2018) proposed a novel method for radial network constraints suitable for the flexible reconstruction of distribution networks. This method significantly enhances the flexibility of the network topology, thereby improving the feasibility and optimality of optimization problems related to reconstruction. Liu et al. (2019b) comprehensively considered proactive fault islanding and restoration. Lei et al. (2020) proposed a novel approach for radiality constraints, which fully enables the topological and some other related flexibilities of systems. However, only adjusting the grid structure is insufficient. The faults caused by the restoration should be inspected and repaired timely to reduce the duration of the faults and power outage. Hence, it is of great significance to consider the dispatching of the repair crews (RCs) to repair and restore the ADN against extreme disasters.

The RCs stand out as crucial resilience enhancement forces that find wide applications in distribution networks. Specifically, RCs play a vital role in facilitating coupling repair and restoration processes. Efficiently dispatching RCs to repair specific damaged components is essential for fully restoring a power grid following disasters, thereby supporting the network restoration of distribution networks (Van Hentenryck et al., 2011; Zhang et al., 2020). Bian et al. (2021) proposed a RC deployment model for fault repair and system restoration by solving a two-stage stochastic optimization problem. Arif et al. (2017) delved into the co-optimization of RC routing and reconfiguration for distribution network restoration. Considering the resource capacity limits, the fault repair and restoration model was proposed by Shi et al. (2022) to optimize the scheduling for RCs to repair faulted lines. Notably, recent studies have explored strategies such as coordinating energy scheduling with dynamic microgrid formation to reduce post-disaster recovery costs and co-optimizing RC routing with ADN reconfiguration for efficient restoration (Yao et al., 2019; Yao et al., 2020). However, existing research often addresses NR and RCs in isolation. Nevertheless, RC dispatching in the aftermath of extreme disasters poses a significant challenge as it involves addressing the combinatorial optimization issues related to depot location, equipment transportation, allocation, and crew assignment (Golshani et al., 2019; Inanlouganji et al., 2022). Thus, how to tackle the coordination between RC dispatching and NR is still a remaining key issue.

However, these works mentioned above still have two challenges to overcome: one challenge is how to enhance the resilience level of the ADN with accurate fault scenarios. The other challenge is how to solve and obtain the NR and RC repair and restoration scheduling for the ADN against extreme disaster scenarios. Based on the above, the contributions of this paper are concluded as follows:

1) The RC dispatching and fault repair sequence model is proposed to reduce the fault time period and the corresponding economic losses under extreme disasters. RC numbers and material capacity limits are modeled as constraints to describe the repair decision, while the fault repair sequence constraints are also integrated in the model to obtain optimal repair scheduling.
2) The RC and NR coordinated ADN operation method is devised to support critical loads and reduce the economic loss during the fault periods. Compared with conventional methods, the proposed method can effectively achieve optimal repair routing and load recovery scheduling for a fast and secure restoration.

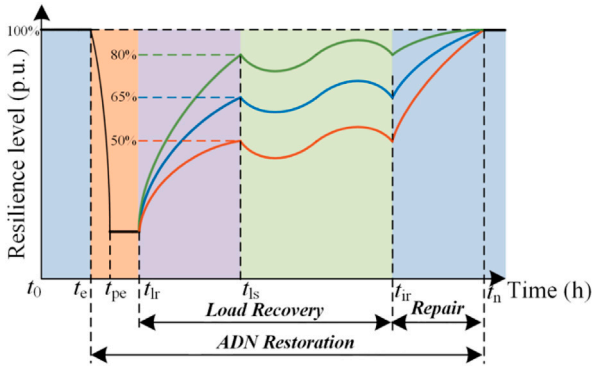

FIGURE 1
Resilience curve and ADN restoration framework.

2 Resilience-oriented ADN restoration framework

The conceptual resilience curve is illustrated in Figure 1. The ADN's resilience level is measured by the ratio of the supplied load. Before and after the extreme event, the ADN typically encompasses five states: pre-event (t_0–t_e), event unfolding ($t_e - t_{pe}$), post-event (t_{pe}–t_{lr}), restoration (t_{lr}–t_{ir}), and post-restoration states (t_{ir}–). These states commonly represent the total energy supplied to the critical loads. In this concept, progression of the MDS during a natural disaster can be explained as follows: in the pre-event state, the ADN can operate in a normal state. When the disaster occurs at t_e, the power supply to loads is disrupted, leading to a decrease in the load supply level (event unfolding state). After the event, the ADN reaches the post-event state at t_{lr}, representing the worst system condition and load recovery initiation in the ADN. As critical loads are gradually restored, the system state progresses toward the next state until the faults are repaired at t_{ir}. After all the faults are repaired, it is ensured that the loads of the ADN recover to the pre-event level. Thus, the ADN gradually returns to the normal state, and the whole process ends.

In this study, we propose a resilience-oriented ADN restoration approach where fault scenarios are generated before extreme events by the proposed fault possibility model. Then, the RC and NR coordinated load restoration problem is solved to obtain the optimal ADN restoration scheduling during the post-event, restoration, and post-restoration states until all the faults are repaired. Hence, the proposed resilience-oriented ADN restoration framework can leverage all the resources, including the power supply, system topology adjustment measures, and RCs, to effectively enhance the resilience level against a disaster.

3 Resilience-oriented ADN restoration model

In this study, in order to supply critical loads, the ADN makes use of strategies such as topology reconfiguration and island partition through the deployment of flexible resources. Furthermore, in the resilience-oriented ADN restoration model, local flexible resources, including controllable diesel generators (DGs), and energy storage systems (ESSs) are utilized with the distributed generation systems, such as photovoltaic (PV) systems and wind turbine (WT) systems, to provide energy to the loads in the ADN. Furthermore, line switches are operated by the DSO for NR by considering the DistFlow power flow model. Additionally, RCs are dispatched to repair the faults with limitations of the numbers and material resources.

3.1 Local flexible resources

Regarding flexible resources, both DGs and ESSs possess flexible capabilities. These are designated as the power source within the isolated islands to provide electricity for shed loads.

3.1.1 Model of the DGs

Distribution grids often rely on controllable distributed power sources, primarily utilizing DGs. DGs are commonly employed in isolated grids that are not connected to the upstream network or used as emergency power sources during grid failures. They can even be utilized in more complex scenarios such as peak shaving and power support. The model of the DGs is given in Eqs. (1)–(3) as follows:

$$-\frac{P_{i,t}^{\mathrm{DG}}\sqrt{1-(\kappa_i)^2}}{\kappa_i^{\mathrm{DG}}} \le Q_{i,t}^{\mathrm{DG}} \le \frac{P_{i,t}^{\mathrm{DG}}\sqrt{1-(\kappa_i)^2}}{\kappa_i^{\mathrm{DG}}},\ \forall t \in \mathrm{N_T}, \forall i \in \mathrm{N_{DG}}, \quad (1)$$

$$\sqrt{\left(P_{i,t}^{\mathrm{DG}}\right)^2 + \left(Q_{i,t}^{\mathrm{DG}}\right)^2} \le S_i^{\mathrm{DG}},\ \forall t \in \mathrm{N_T}\ , \forall i \in \mathrm{N_{DG}}, \quad (2)$$

$$P_{min}^{\mathrm{DG}} \le P_{i,t}^{\mathrm{DG}} \le P_{max}^{\mathrm{DG}},\quad \forall t \in \mathrm{N_T}, \forall i \in \mathrm{N_{DG}}, \quad (3)$$

where $P_{i,t}^{\mathrm{DG}}$ and $Q_{i,t}^{\mathrm{DG}}$ are the active and reactive power generation of the DG at node i at time t, respectively; κ_i^{DG} is the power factor of the DG; S_i^{DG} denotes the DG capacity at node i; and P_{min}^{DG} and P_{max}^{DG} are the lower and upper limits of the output power generation of the DG, respectively.

3.1.2 Model of the ESSs

ESSs provide possibility and solutions for post-disaster emergency dispatch in distribution networks. They can act as a fast reserve to effectively support regional control, scheduled dispatch, frequency regulation, and peak shaving. In the distribution phase, the introduction of energy storage devices can effectively mitigate the fluctuation between uncontrollable distributed power generation and load demand. ESSs interact with the grid by controlling the charging and discharging of batteries based on received control commands. Additionally, the inverters of the ESSs have a certain reactive power support capability, providing voltage support to blackout nodes according to the operational requirements of the grid. Detailed model of the ESSs are given in Eqs. (4)–(9).

$$E_{i,t}^{\mathrm{ESS}} = E_{i,t-1}^{\mathrm{ESS}}\left(1 - A_i^{\mathrm{ESS}}\right) + P_{i,t}^{\mathrm{ESSC}}\eta^{\mathrm{C}}\Delta t - \frac{P_{i,t}^{\mathrm{ESSD}}}{\eta^{\mathrm{D}}\Delta t},\ \forall t \in \mathrm{N_T}, \forall i \in \mathrm{N_{ESS}}, \quad (4)$$

$$0 \le P_{i,t}^{\mathrm{ESSC}} \le P_{max}^{\mathrm{ESS}} \cdot S_{i,t}^{\mathrm{ESSC}},\quad \forall t \in \mathrm{N_T}, \forall i \in \mathrm{N_{ESS}}, \quad (5)$$

$$0 \le P_{i,t}^{\mathrm{ESSD}} \le P_{max}^{\mathrm{ESS}} \cdot S_{i,t}^{\mathrm{ESSD}},\quad \forall t \in \mathrm{N_T}, \forall i \in \mathrm{N_{ESS}}, \quad (6)$$

$$E_{min}^{\mathrm{ESS}} \le E_{i,t}^{\mathrm{ESS}} \le E_{max}^{\mathrm{ESS}},\quad \forall t \in \mathrm{N_T}, \forall i \in \mathrm{N_{ESS}}, \quad (7)$$

$$S_{i,t}^{\mathrm{ESSC}} + S_{i,t}^{\mathrm{ESSD}} \le 1,\ \forall t \in \mathrm{N_T},\ \forall i \in \mathrm{N_{ESS}}, \quad (8)$$

$$\sqrt{\left(P_{i,t}^{\mathrm{ESS}}\right)^2+\left(Q_{i,t}^{\mathrm{ESS}}\right)^2}\le S_i^{\mathrm{ESS}},\quad \forall t\in \mathrm{N_T},\forall i\in \mathrm{N_{ESS}}, \tag{9}$$

where $E_{i,t}^{\mathrm{ESS}}$ represents the SOC of the ESS at time t at node i; A_i^{ESS} is the loss coefficient of the ESS; $P_{i,t}^{\mathrm{ESSC}}$, $P_{i,t}^{\mathrm{ESSD}}$, and $P_{i,t}^{\mathrm{ESS}}$ are the charging, discharging, and the net ESS power injection into node i at time t, respectively; η^{C} and η^{D} are the charging and discharging efficiencies of the ESS, respectively; $S_{i,t}^{\mathrm{ESSC}}$ and $S_{i,t}^{\mathrm{ESSD}}$ denote the charging and discharging binary status, respectively; P_{max}^{ESS} is the upper limit of the ESS charging and discharging power limit; S_{min}^{ESS} and S_{max}^{ESS} are the SOC limits of the ESS; S_i^{ESS} is the capacity of the ESS; and $Q_{i,t}^{\mathrm{ESS}}$ is the reactive power of the ESS.

3.1.3 Model of the RES

Distributed RES can also be utilized to support the ADN resilience level. The corresponding model of the RES generation are represented in Eqs. (10)–(12) as follows:

$$-\frac{P_{i,t}^{\mathrm{RES}}\sqrt{1-(\kappa_i)^2}}{\kappa_i^{\mathrm{RES}}}\le Q_{i,t}^{\mathrm{RES}}\le\frac{P_{i,t}^{\mathrm{RES}}\sqrt{1-(\kappa_i)^2}}{\kappa_i^{\mathrm{RES}}},\ \forall t\in \mathrm{N_T},\forall i\in \mathrm{N_{PV}}\bigcup \mathrm{N_{WT}}, \tag{10}$$

$$\sqrt{\left(P_{i,t}^{\mathrm{RES}}\right)^2+\left(Q_{i,t}^{\mathrm{RES}}\right)^2}\le S_i^{\mathrm{RES}},\ \forall t\in \mathrm{N_T},\forall i\in \mathrm{N_{PV}}\bigcup \mathrm{N_{WT}}, \tag{11}$$

$$0\le P_{i,t}^{\mathrm{RES}}\le P_{max}^{\mathrm{RES}},\mathrm{RES}\in\{\mathrm{PV},\mathrm{WT}\},\forall t\in \mathrm{N_T},\forall i\in \mathrm{N_{PV}}\bigcup \mathrm{N_{WT}}, \tag{12}$$

where $P_{i,t}^{\mathrm{RES}}$ and $Q_{i,t}^{\mathrm{RES}}$ are the active and reactive power generation of the PVs and WTs at time t at node i, respectively; κ_i^{RES} is the power factor of PVs and WTs; S_i^{RES} denotes the RES capacity at node i; and P_{max}^{RES} is the maximal power limit of the PVs and WTs.

3.2 DistFlow model of the ADN

The DistFlow model (Baran and Wu, 1989a) is typically used in the literature for simplifying the power flow equations to make them more tractable for analysis. This simplification, while enabling easier computation, can lead to inaccuracies in modeling the real behavior of the electrical distribution network, particularly under heavy loading conditions or when dealing with complex network topologies. Furthermore, the DistFlow model is primarily designed for radial distribution networks, which can be formulated as Eqs. (13)–(16):

$$\begin{cases}\sum_{k\in a(i)}P_{ki,t}^{\mathrm{line}}-r_{ki}I_{ki,t}^2=\sum_{j\in b(i)}P_{ij,t}^{\mathrm{line}}+P_{i,t},\\ \sum_{k\in a(i)}Q_{ki,t}^{\mathrm{line}}-x_{ki}I_{ki,t}^2=\sum_{j\in b(i)}Q_{ij,t}^{\mathrm{line}}+Q_{i,t},\end{cases}\ \forall t\in \mathrm{N_T},\forall ij\in\mathcal{B}, \tag{13}$$

$$U_{j,t}^2=U_{i,t}^2-2\left(r_{ij}P_{ij,t}^{\mathrm{line}}+x_{ij}Q_{ij,t}^{\mathrm{line}}\right)+\left(r_{ij}^2+x_{ij}^2\right)I_{ij,t}^2,\ \forall t\in \mathrm{N_T},\forall ij\in\mathcal{B}, \tag{14}$$

$$I_{ij,t}^2=\frac{\left(P_{ij,t}^{\mathrm{line}}\right)^2+\left(Q_{ij,t}^{\mathrm{line}}\right)^2}{U_{i,t}^2},\ \forall t\in \mathrm{N_T},\forall ij\in\mathcal{B}, \tag{15}$$

$$U_{i,t}^{\min}\le U_{i,t}\le U_{i,t}^{\max},\ \forall t\in \mathrm{N_T}, \tag{16}$$

where $P_{ij,t}^{\mathrm{line}}$ and $Q_{ij,t}^{\mathrm{line}}$ are the active and reactive power on branch ij in the branch set $\mathcal{B}$ over a time period t, respectively; r_{ki} and x_{ki} are the resistance and reactance parameters of branch ki, respectively; $I_{ki,t}$ is the current through branch ki; $a(i)$ is the set of ancestor nodes; $b(i)$ is the set of child nodes; and $U_{i,t}$ is the voltage of node i at time t, which is within the range of the minimal limit $U_{i,t}^{\min}$ and the maximal limit $U_{i,t}^{\max}$.

In addition, $P_{i,t}$ and $Q_{i,t}$ represent the active and reactive power injections, respectively, which can be formulated as in the Eq. (17).

$$\begin{cases}P_{i,t}=P_{i,t}^{\mathrm{DG}}+P_{i,t}^{\mathrm{PV}}+P_{i,t}^{WT}+P_{i,t}^{\mathrm{ESSD}}-P_{i,t}^{\mathrm{ESSC}}-\lambda_iP_{i,t}^{\mathrm{load}},\\ Q_{i,t}=Q_{i,t}^{\mathrm{DG}}+Q_{i,t}^{\mathrm{PV}}+Q_{i,t}^{\mathrm{ESS}}-\lambda_iQ_{i,t}^{\mathrm{load}},\end{cases},\forall t\in \mathrm{N_T}, \tag{17}$$

where λ_i denotes the binary load state of node i; $P_{i,t}^{\mathrm{load}}$ and $Q_{i,t}^{\mathrm{load}}$ are the active and reactive power loads, respectively.

3.3 Model of RC dispatching and fault repair

In response to natural disasters and power line faults, the power grid needs to sequentially repair each affected line to shorten the damage period. It is crucial to find the optimal maintenance sequence within the fault period. The method for optimizing the fault repair strategy involves the introduction of a series of constraints to the switch status variables during network restructuring and island partitioning. These constraints are integrated into a unified model for fault recovery during the restructuring and islanding process. When faults occur, it ensures that the lines remain disconnected. At the same time, it is restricted to restoring a maximum of h faulty lines. The constraints on the open/close status of the faulty lines in the model represent the maintenance strategy given in Eqs. (18), (19) as follows:

$$\alpha_{ij}^0=0,\quad \forall ij\in\mathcal{B}_{\mathrm{F}}, \tag{18}$$

$$\alpha_{ij}^{t_n}\le\alpha_{ij}^{t_m},\quad \forall ij\in\mathcal{B}_{\mathrm{F}},t_n\le t_m, \tag{19}$$

$$\sum_F\alpha_{ij}^{t+T_f}-\sum_F\alpha_{ij}^t\le h,\quad \forall ij\in\mathcal{B}_{\mathrm{F}},\forall t\in \mathrm{N_T}, \tag{20}$$

where α_{ij}^t is the line switch status of branch ij in the fault branch set $\mathcal{B}_{\mathrm{F}}$; h represents the maximum number limit of the power lines that can be simultaneously repaired at a time period; and T_f denotes the fault repair time. Equation 18 describes the initial state when faults occur; all fault lines are in the open state. Equation 19 represents that the fault line should be repaired only once. Equation 20 ensures that during the fault recovery process, a maximum of h faulty lines can be repaired at each time period.

Resource availability is ensured by Eq. (21), which stipulates that the resource capacity of each crew should be sufficient to meet the total resource demand of the damaged components in its assigned route:

$$\sum_{m\in M}\sum_F Y_{ij,\tau}^{RC}\cdot rm_{ij}^m\le RS_\tau^m,\forall\tau\in\Xi,\ \forall ij\in\mathcal{B}_{\mathrm{F}}, \tag{21}$$

where $Y_{ij,\tau}^{RC}$ denotes the binary variable, which equals 1 if the fault line $ij\in\mathcal{B}_{\mathrm{F}}$ is fixed by the crew team τ in the RC team set Ξ; rm_{ij}^m represents the required mth kind of material to repair the fault line $ij\in\mathcal{B}_{\mathrm{F}}$; and RS_τ^m represents the capacity limit of the crew team τ with the mth kind of material.

3.4 Radial operation constraints of the ADN

The ADN must satisfy the following radial constraints which can be formulated as Eqs. (22)–(25):

$$\alpha_{ij} = \mu_{ij} + \nu_{ij}, \tag{22}$$

$$\sum_{ij\in\Omega_{i,A}}\mu_{ij} + \sum_{ij\in\Omega_{i,C}}\nu_{ij} = 1, \quad \forall i \in \Omega_n, \tag{23}$$

$$\sum_{ij\in\Omega_{i,A}}\mu_{ij} + \sum_{ij\in\Omega_{i,C}}\nu_{ij} = 0, \quad \forall i \in \Omega_s, \tag{24}$$

$$\alpha_{ij} \in \{0,1\}, \mu_{ij} \in \{0,1\}, \nu_{ij} \in \{0,1\}, \tag{25}$$

where μ_{ij} and ν_{ij} are the binary variables representing the virtual power flow directions of branch ij, with $\mu_{ij} = 1$ indicating the default power flow direction and $\nu_{ij} = 1$ indicating the inverse power flow direction; Ω_n is the set of normal nodes; Ω_s is the set of alternative island source nodes; $\Omega_{i,A}$ is the set of branches with i as the ancestor node; and $\Omega_{i,C}$ is the set of branches with i as the child node.

4 Resilience-oriented RC and NR coordinated operational scheduling method

4.1 Model reformulation

4.1.1 Big M method

With the Big M method, the Eq. 14 can beeformulated into the following constraints in Eqs. (26)–(30):

$$\mathrm{M}\alpha_{ij} \le P^{\mathrm{line}}_{ij,t} \le \mathrm{M}\alpha_{ij}, \quad \forall t \in \mathrm{N_T}, \forall ij \in \mathcal{B}, \tag{26}$$

$$-\mathrm{M}\alpha_{ij} \le Q^{\mathrm{line}}_{ij,t} \le \mathrm{M}\alpha_{ij}, \quad \forall t \in \mathrm{N_T}, \forall ij \in \mathcal{B}, \tag{27}$$

$$0 \le I^2_{ij,t} \le \mathrm{M}\alpha_{ij}, \ \forall t \in \mathrm{N_T}, \forall ij \in \mathcal{B}, \tag{28}$$

$$U^2_{j,t} - U^2_{i,t} + 2\left(r_{ij}P^{\mathrm{line}}_{ij,t} + x_{ij}Q^{\mathrm{line}}_{ij,t}\right) - \left(r^2_{ij} + x^2_{ij}\right)I^2_{ij,t} - \mathrm{M}\left(1-\alpha_{ij}\right) \le 0, \ \forall t \in \mathrm{N_T} \forall ij \in \mathcal{B}, \tag{29}$$

$$U^2_{j,t} - U^2_{i,t} + 2\left(r_{ij}P^{\mathrm{line}}_{ij,t} + x_{ij}Q^{\mathrm{line}}_{ij,t}\right) - \left(r^2_{ij} + x^2_{ij}\right)I^2_{ij,t} + \mathrm{M}\left(1-\alpha_{ij}\right) \ge 0, \ \forall t \in \mathrm{N_T}, \forall ij \in \mathcal{B}, \tag{30}$$

where M is a big enough positive number.

4.1.2 SOCP relaxation of the DistFlow power flow model

A new set of variables $\mathcal{U}_{i,t}$ and $\mathcal{I}_{ij,t}$ are presented to replace the voltage and current as Eqs. (31)–(33):

$$\begin{cases} \mathcal{U}_{i,t} = U^2_{i,t} \\ \mathcal{I}_{ij,t} = I^2_{ij,t} \end{cases}, \ \forall t \in \mathrm{N_T}, \forall ij \in \mathcal{B}, \tag{31}$$

$$\mathcal{I}_{ij,t} \ge \frac{\left(P^{\mathrm{line}}_{ij,t}\right)^2 + \left(Q^{\mathrm{line}}_{ij,t}\right)^2}{\mathcal{U}_{i,t}}, \ \forall t \in \mathrm{N_T}, \forall ij \in \mathcal{B}, \tag{32}$$

$$\left\| \begin{matrix} 2P^{\mathrm{line}}_{ij,t} \\ 2Q^{\mathrm{line}}_{ij,t} \\ \mathcal{I}_{ij,t} - \mathcal{U}_{i,t} \end{matrix} \right\|_2 \le \mathcal{I}_{ij,t} + \mathcal{U}_{i,t}, \ \forall t \in \mathrm{N_T}, \forall ij \in \mathcal{B}. \tag{33}$$

Based on above, the relaxation gap of the DistFlow model can be defined as Eq. (34).

$$gap_{ij,t} = \left| \mathcal{I}_{ij,t} - \frac{\left(P^{\mathrm{line}}_{ij,t}\right)^2 + \left(Q^{\mathrm{line}}_{ij,t}\right)^2}{\mathcal{U}_{i,t}} \right|, \ \forall t \in \mathrm{N_T}, \forall ij \in \mathcal{B}. \tag{34}$$

4.1.3 SOCP relaxation of the DG and ESS

Similar to the relaxation of the DistFlow model, the SOCP relaxation of the DG and ESS are given as Eqs. (35), (36).

$$\left\| \begin{matrix} P^{\mathrm{DG}}_{i,t} \\ Q^{\mathrm{DG}}_{i,t} \end{matrix} \right\| \le S^{\mathrm{DG}}_i, \ \forall t \in \mathrm{N_T}, \tag{35}$$

$$\left\| \begin{matrix} P^{\mathrm{ESS}}_{i,t} \\ Q^{\mathrm{ESS}}_{i,t} \end{matrix} \right\| \le S^{\mathrm{ESS}}_i, \ \forall t \in \mathrm{N_T}. \tag{36}$$

4.2 Objective function

The objective function of RCs repair and system restoration is formulated as Eq. (37).

$$\mathcal{O} = \sum_{t=1}^{\mathrm{N_T}}\left(\sum_{i=1}^{\Omega_{\mathrm{ADN}}}\theta_i\,(1-\lambda_i)P^{\mathrm{load}}_{i,t} + \sum_{i=1}^{\mathrm{N_{DG}}}C^{\mathrm{DG}}P^{\mathrm{DG}}_{i,t} + \sum_{i=1}^{\mathrm{N_{ESS}}}C^{\mathrm{ESS}}P^{\mathrm{ESS}}_{i,t} + \sum_{i=1}^{\mathrm{N_{PV}}}C^{\mathrm{PV}}P^{\mathrm{PV}}_{i,t} + \sum_{i=1}^{\mathrm{N_{WT}}}C^{\mathrm{WT}}P^{\mathrm{WT}}_{i,t}\right), \tag{37}$$

where θ_i is the importance coefficient of the load at node i, which can be evaluated by the value of the lost load (Kariuki and Allan, 1996); C^{DG}, C^{PV}, C^{WT}, and C^{ESS} are the operational costs of DG, PV, WT, and ESS, respectively.

4.3 RC and NR coordinated ADN restoration method

After the above steps, the overall RC and NR coordinated ADN restoration model can be solved using a commercial solver. Figure 2 shows the flowchart of the proposed method.

5 Case studies

To evaluate the proposed method, the IEEE 33 bus active distribution system is used (Baran and Wu, 1989b). System configuration is shown in Figure 3. Five WTs, three PVs, one set of DGs, and one ESS are integrated into the ADN. Time duration and equipment configuration parameters for the fault scenario are listed in Table 1 and Table 2, respectively. Figure 4 shows the predicted power generation curve of the PVs and WTs. The problem is solved using the MATLAB R2018b platform with Gurobi 10.0.0 (Gurobi Optimization and LLC, 2023). The results demonstrate that our approach can achieve optimal load recovery strategies within 226 s, which is computationally feasible in real-world applications.

5.1 Network reconfiguration and fault repair scheduling results

To show the importance of NR and RC coordinated resilience dispatching, the ADN topologies during the fault duration are established, as illustrated in Figures 5A–F. As mentioned in Table 1, initially, at 8:00, there are six faults in branches 6, 12, 18, 21, 24, and 32, which are marked in red in Figure 5A.

During the first fault duration period 8:00–9:00, the ADN is reconfigured into three islands as the temporary status for resilience

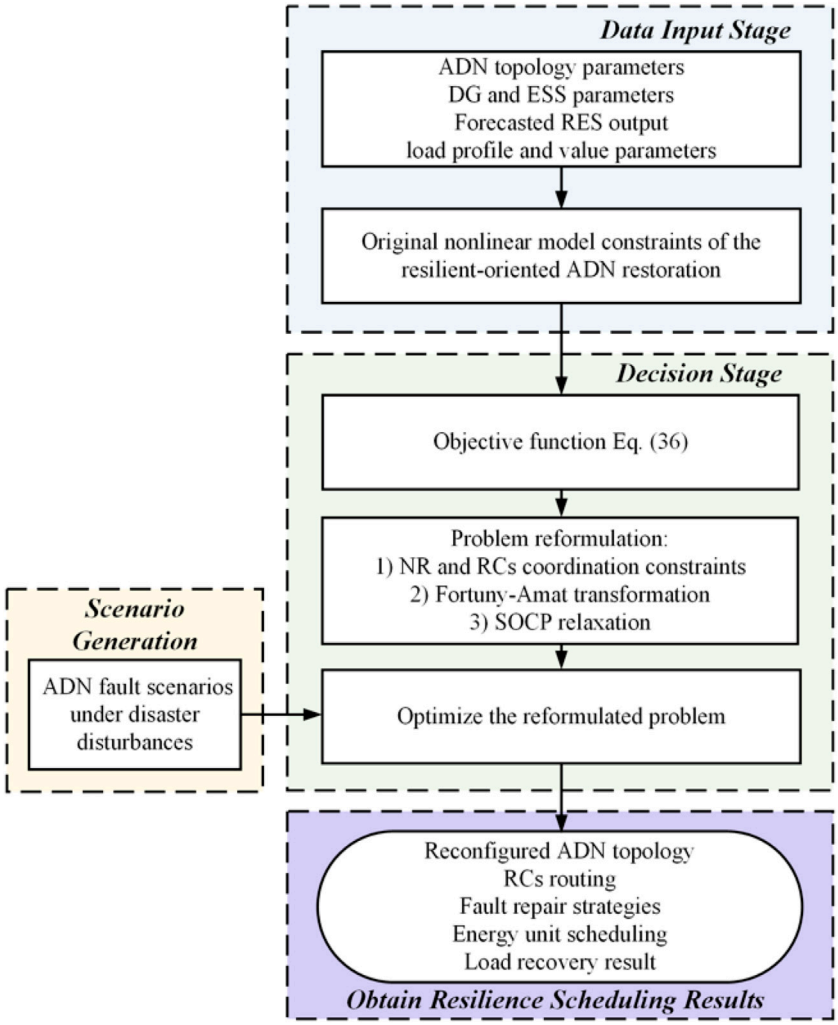

FIGURE 2
Flowchart of the RC and NR coordinated ADN restoration method.

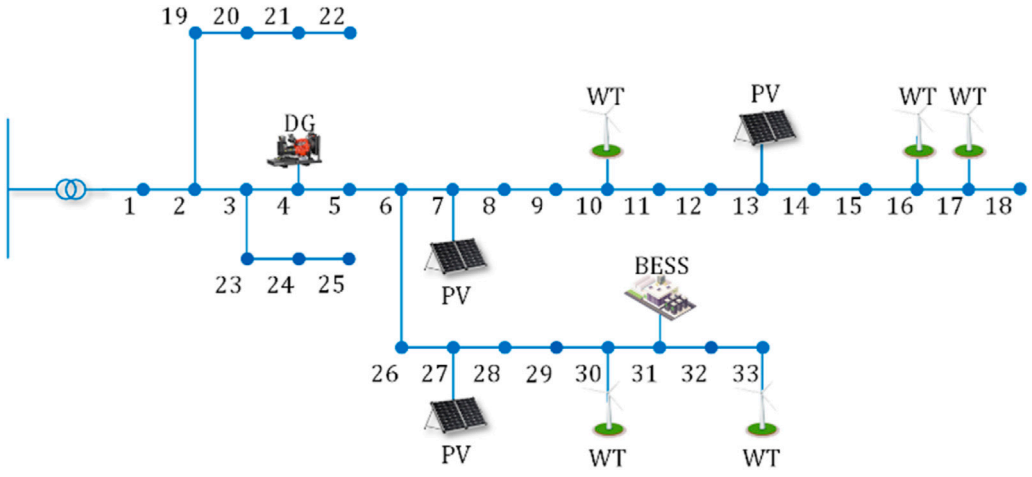

FIGURE 3
System configuration of the case study.

10.3389/fenrg.2024.1369452

TABLE 1 Fault scenario parameters.

Fault branch	Branch 6 (nodes 2–19)	Branch 12 (nodes 12 and 13)	Branch 18 (nodes 2–19)	Branch 21 (nodes 21 and 22)	Branch 24 (nodes 24 and 25)	Branch 32 (nodes 32 and 33)
Time duration	8:00–14:00	8:00–14:00	8:00–14:00	8:00–14:00	8:00–14:00	8:00–14:00

TABLE 2 Energy equipment configuration parameters.

Equipment	Location	Capacity
PV	Node 7	500 kVA
	Node 13	300 kVA
	Node 27	400 kVA
WT	Node 10	500 kVA
	Node 16	300 kVA
	Node 17	200 kVA
	Node 30	200 kVA
	Node 33	300 kVA
DG	Node 4	200 kWh
ESS	Node 31	500 kWh

operation. Nodes 1–6, 23–24, and 26 are in the first island that is connected to the upstream network and the DG to supply the demand. Nodes 7–8 and 19–21 are in the second island to support the local power demand using PVs in node 7. Nodes 9–18, 22, 25, and 27–33 are divided into the third island, with five WTs and the BESS in node 31 for resilience operation. In addition to the normal power line branches, four power-tie lines are all deployed to further improve the power exchange ability in the ADN to enhance the resilience level. Meanwhile, RCs are all scheduled to start the repair process of the fault lines between nodes 6–7 and nodes 12–13, which can be illustrated in the next fault duration.

During the second fault duration period 9:00–10:00, in Figure 5B, the fault in the branches between nodes 6–7 and nodes 12–13 are repaired, respectively. Then, the ADN is reconfigured into two islands for resilience enhancement. Nodes 1–11, 19–21, and 23–33 in the first island are meant to support critical loads supplied by the main grid, the DG, five WTs, two PVs, and the BESS. The second island includes nodes 12–14 and 22 to support the local power demand using the PV in node 13. Similar to the situation during the fault duration period 8:00–9:00, the four power tie line branches are all still kept closed to enhance the resilience level. Meanwhile, the RCs are all scheduled to start the fault line repair process between nodes 24 and 25.

For the third fault duration period 10:00–11:00 (Figure 5C), the fault in the branches between nodes 24 and 25 is repaired by the RCs. Hence, the ADN is mitigated into a radial network topology with all the energy units engaged. Different from the situation before, the power tie line between nodes 25 and 29 is kept open to avoid the loop circuit in the ADN.

Figure 5D shows the ADN topology during the fourth fault duration period 11:00–12:00. The RCs repaired the fault line between nodes 2 and 19, which contributes to the improvement in the ADN resilience level by increasing the power exchange ability in the network. It should be noted

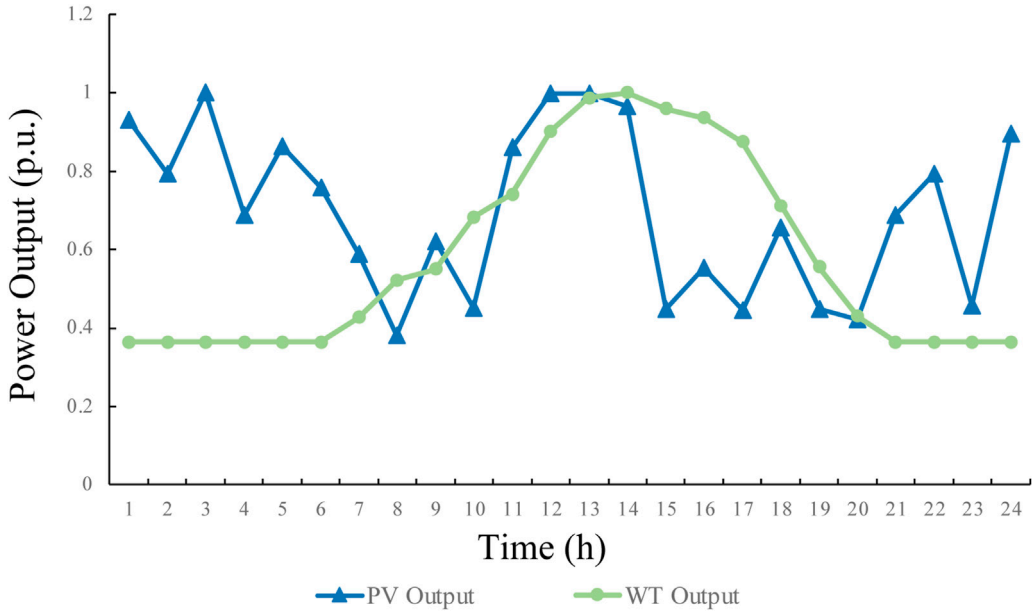

FIGURE 4
Predicted power generation of the WTs and PVs in p.u.

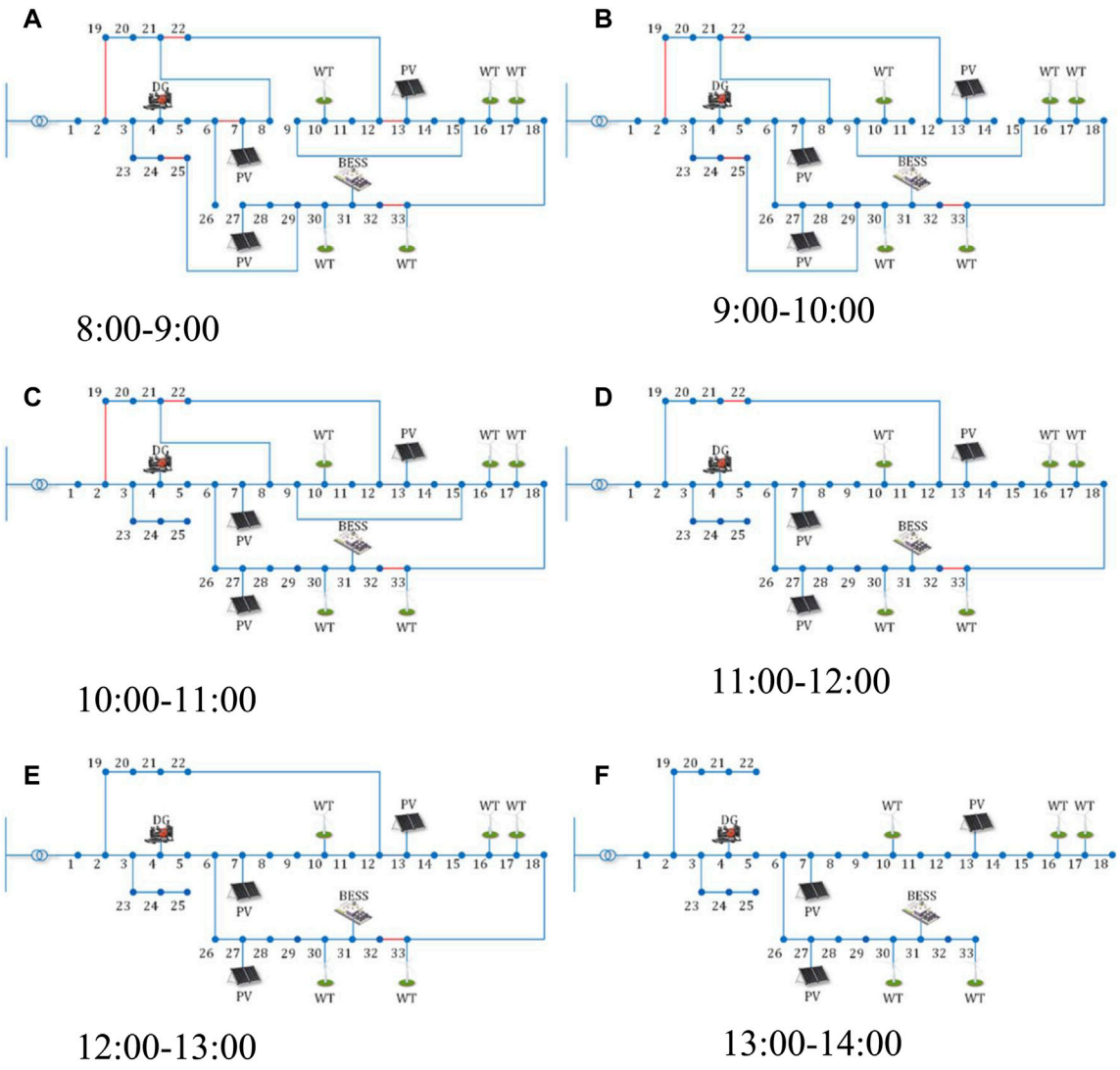

FIGURE 5
Network reconfiguration and the fault repair scheduling results of the ADN.

that constrained by the radial network topology, the power tie line between nodes 9 and 15 is opened. RCs are scheduled to start the fault line repair process between nodes 21 and 22.

Finally, as shown in Figures 5E, F, in the last duration period 12: 00–14:00, the RCs repaired the last fault line between nodes 32 and 33, and after the repair process, the ADN is restored to the normal mode topology, ensuring that the system resilience level achieves a 100% recovery. Hence, the proposed NR and RC coordinated operation model can effectively improve the system resilience level by repairing the faults and operating the power line switches using the optimal strategy.

5.2 Load recovery and voltage management results

Regarding the improvement in the resilience level of the ADN, Figure 6 illustrates the resilience level and the lost load, the preserved load, and total load demands. It can be concluded that the resilience level of the ADN is improved from 37% at 8: 00 to 100% at 14:00, which indicates that the NR and RC can effectively reduce load shedding. Furthermore, by repairing faults lines, the resilience level is improved by 30%, 23%, 7%, 2%, and 1%. This indicates that the optimal RC scheduling strategy can effectively obtain the maximal resilience level improvement during every repair process. Meanwhile, the decline in the lost load demand and the increase in the preserved load also prove that the proposed NR and RC coordinated operation method can effectively improve the system resilience level and eventually restore the ADN to the normal status.

Figure 7 shows the nodal voltages of the ADN at each time slot. The nodal voltages are measured by the per-unit value by setting the voltage base values to 12.66 kV. The maximum and the minimum voltages are 1.05 and 0.95, respectively. The nodal voltage is acceptable in practice, considering that the voltage limits are 0.9–1.1 p.u. It should be noted that after the repair of fault lines in each duration period, the nodal voltages in the ADN are improved to be closer to the base value, which illustrates that the proposed method can effectively secure ADN operation with the optimal repair strategy.

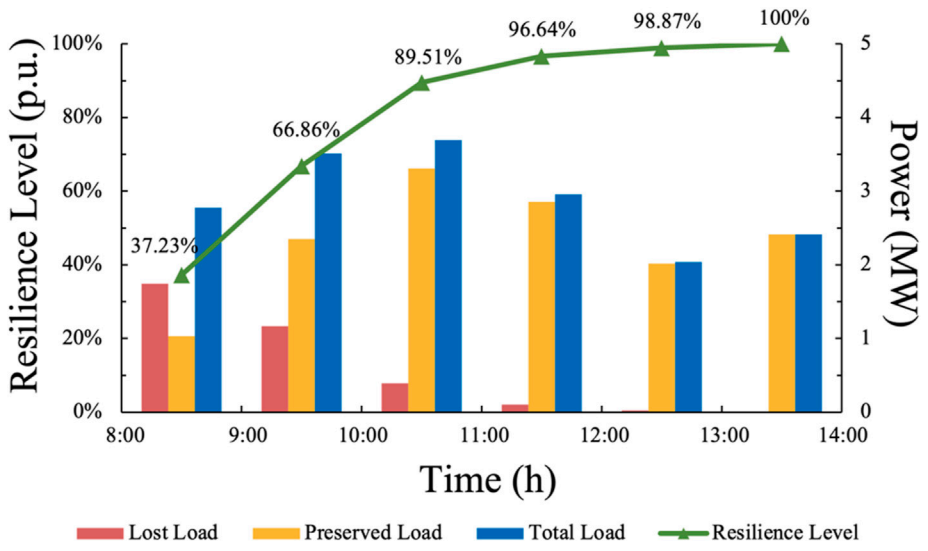

FIGURE 6
Resilience level and load preserve in the ADN (in p.u.).

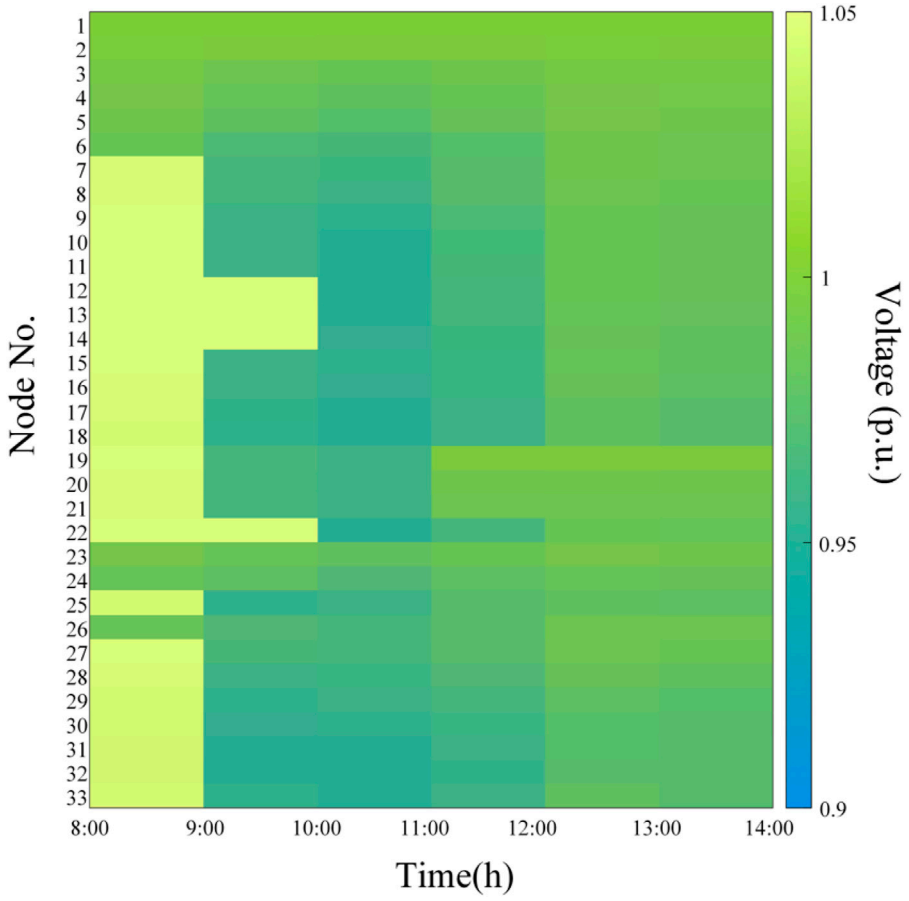

FIGURE 7
Voltage management in the ADN (in p.u.).

TABLE 3 Result comparison.

Result	Method #1	Method #2	Method #3
Load shedding loss (US$)	32,838.17	16,698.05	10,734.38
Operational cost (US$)	1,198.92	2,332.54	3,791.08
Total cost (US$)	34,037.09	19,030.59	14,525.46

5.3 Result comparison

To further evaluate the proposed model and method, three methods are compared as follows:

Method #1—NR method: Only NR is considered in this method to support the load demand, and all faults are repaired at the end of the fault duration.

Method #2—NR operation method with a fixed repair sequence: The ADN resilience level is enhanced using the NR operation method, and the fault lines are repaired using a fixed sequence with the distance measured between the fault lines and node 1 in the ADN.

Method #3—NR and RC scheduling coordinated operation method: Three groups of RCs are scheduled to repair the fault lines simultaneously with NR of the ADN.

From Table 3, it can be concluded that the load shedding loss of **Method #1** is larger than those of **Method #2** and **Method #3** with gaps of $16,140.12 and $5,963.67, respectively. This is because in **Method #1**, the RC repair capability is not considered. All the faults are repaired until the end of the fault duration, which weakens the power supply capacity of the ADN. In **Method #2**, the RCs only repair the fault lines by following the geographical distance sequence, which may lead to suboptimal scheduling routing and the increase in economic losses. Among the three approaches, **Method #3** can obtain the minimal load shedding loss.

The operational cost to reduce carbon emissions increases from $1,198.92 in **Method #1** to $2,332.54 and $3,791.08 in **Method #2** and **Method #3**, respectively. This is tenable since with NR and RC coordination, more nodes in the ADN and in the same island are connected with the DG, which leads to an increase in the fuel cost of the DG.

Meanwhile, despite the increase in the operational cost of **Method #3**, the total costs of the three methods are $34,037.09, $19,030.59, and $14,525.46, respectively. Therefore, the proposed **Method #3** achieves the best performance in reducing the total cost of load shedding and system operation. Thus, the resilience of the ADN is effectively enhanced, and the proposed NR and RC coordinated method can reduce the economic loss caused by disasters.

6 Conclusion

In this paper, a resilience-oriented operational scheduling method is proposed by coordinating RCs and NR within an ADN to effectively counteract faults. Compared to traditional methods, this method not only establishes power supply islands but also ensures continuous power delivery to critical loads during blackouts by strategically deploying local and external resilience resources and RCs. The synergy between NR and RCs is meticulously orchestrated to simultaneously determine the repair sequence of fault lines and the reconfiguration of the ADN topology. The effectiveness of our approach is demonstrated through numerical simulations, highlighting its superiority in enhancing system resilience and minimizing economic losses when compared to traditional grid recovery methods. Our findings affirm that the coordinated optimization of RC scheduling and NR actions significantly improves the system's resilience. Furthermore, the integration of renewable energy sources and storage systems within the proposed framework could offer benefits to optimize system resilience. Future investigations can be conducted to explore the AI techniques, such as deep reinforcement learning, for further reducing the computation time, which is critical for NR following disasters.

Data availability statement

The raw data supporting the conclusion of this article will be made available by the authors, without undue reservation.

Author contributions

FZ: data curation, investigation, methodology, writing–original draft, and writing–review and editing. PZ: conceptualization, validation, and writing–original draft. TS: conceptualization, formal analysis, visualization, writing–original draft, and writing–review and editing. JJ: funding acquisition, project administration, and writing–original draft. GL: data curation, investigation, and writing–original draft. SX: investigation, methodology, validation, and writing–original draft. JZ: writing–original draft and writing–review and editing. KY: investigation, writing–original draft, and writing–review and editing.

Funding

The author(s) declare that financial support was received for the research, authorship, and/or publication of this article. This work was financially supported by the Science and Technology Project of State Grid Jiangsu Electric Power Co., Ltd. (J2023098, Research and Application of Construction Technology of the Power Outage Information Resource Pool in the Active Distribution Network Based on Multi-source Sensing and Dynamic Topology Analysis).

Conflict of interest

Authors FZ, SX, JZ, and KY were employed by State Grid Suqian Power Supply Company. Authors PZ and GL were employed by State Grid Xuzhou Power Supply Company. Author JJ was employed by State Grid Jiangsu Electric Power Co., Ltd.

The authors declare that this study received funding from Science and Technology Project of State Grid Jiangsu Electric Power Co., Ltd. The funder had the following involvement in the study: study design, data collection and decision to publish.

The remaining author declares that the research was conducted in the absence of any commercial or financial relationships that could be construed as a potential conflict of interest.

Publisher's note

References

Arif, A., Wang, Z., Wang, J., and Chen, C. (2017). Power distribution system outage management with co-optimization of repairs, reconfiguration, and DG dispatch. *IEEE Trans. Smart Grid* 9 (5), 4109–4118. doi:10.1109/tsg.2017.2650917

Baran, M. E., and Wu, F. F. (1989a). Network reconfiguration in distribution systems for loss reduction and load balancing. *IEEE Trans. Power Deliv.* 4 (2), 1401–1407. doi:10.1109/61.25627

Baran, M. E., and Wu, F. F. (1989b). Network reconfiguration in distribution systems for loss reduction and load balancing. *IEEE Trans. Power Deliv.* 4 (2), 1401–1407. doi:10.1109/61.25627

Bian, Y., Bie, Z., and Li, G. (2021). Proactive repair crew deployment to improve transmission system resilience against hurricanes. *Transm. Distribution* 15 (5), 870–882. doi:10.1049/gtd2.12065

Demetriou, P., Kyriacou, A., Kyriakides, E., and Panayiotou, C. (2016). "Applying exact MILP formulation for controlled islanding of power systems," in 51st International Universities Power Engineering Conference, Coimbra, Portugal, 6-9 September 2016.

Golshani, A., Sun, W., Zhou, Q., Zheng, Q. P., and Hou, Y. (2019). Incorporating wind energy in power system restoration planning. *IEEE Trans. Smart Grid* 10 (1), 16–28. doi:10.1109/tsg.2017.2729592

Gurobi Optimization, LLC (2023). *Gurobi optimizer version 10.0.0*. Available at: https://www.gurobi.com/downloads/gurobi-software (assessed November 23, 20).

Hafez, A. A., Omran, W. A., and Higazi, Y. G. (2018). A decentralized technique for autonomous service restoration in active radial distribution networks. *IEEE Trans. Smart Grid* 9 (3), 1911–1919. doi:10.1109/tsg.2016.2602541

Hou, H., Tang, J., Zhang, Z., Wang, Z., Wei, R., Wang, L., et al. (2023). Resilience enhancement of distribution network under typhoon disaster based on two-stage stochastic programming. *Appl. Energy* 338, 120892. doi:10.1016/j.apenergy.2023.120892

Hou, H., Zhu, S., Geng, H., Li, M., Xie, Y., Zhu, L., et al. (2021). Spatial distribution assessment of power outage under typhoon disasters. *Int. J. Electr. Power and Energy Syst.* 132, 107169. doi:10.1016/j.ijepes.2021.107169

Hussain, A., Bui, V. H., and Kim, H. M. (2019). Microgrids as a resilience resource and strategies used by microgrids for enhancing resilience. *Appl. energy* 240, 56–72. doi:10.1016/j.apenergy.2019.02.055

Inanlouganji, A., Pedrielli, G., Reddy, T. A., and Tormos Aponte, F. (2022). A computational approach for real-time stochastic recovery of electric power networks during a disaster. *Transp. Res. Part E Logist. Transp. Rev.* 163, 102752. doi:10.1016/j.tre.2022.102752

Kariuki, K. K., and Allan, R. N. (1996). Evaluation of reliability worth and value of lost load. *IEE proceedings-Generation, Transm. distribution* 143 (2), 171–180. doi:10.1049/ip-gtd:19960191

Konakalla, S. A. R., Valibeygi, A., and de Callafon, R. A. (2019). Microgrid dynamic modeling and islanding control with synchrophasor data. *IEEE Trans. Smart Grid* 11 (1), 905–915. doi:10.1109/tsg.2019.2948815

Lei, S., Chen, C., Song, Y., and Hou, Y. (2020). Radiality constraints for resilient reconfiguration of distribution systems: formulation and application to microgrid formation. *IEEE Trans. Smart Grid* 11 (5), 3944–3956. doi:10.1109/tsg.2020.2985087

Li, P., Ji, H., Wang, C., Zhao, J., Song, G., Ding, F., et al. (2017). Coordinated control method of voltage and reactive power for active distribution networks based on soft open point. *IEEE Trans. Sustain. Energy* 8 (4), 1430–1442. doi:10.1109/tste.2017.2686009

Liu, J., Qin, C., and Yu, Y. (2019a). Enhancing distribution system resilience with proactive islanding and RCS-based fast fault isolation and service restoration. *IEEE Trans. Smart Grid* 11 (3), 2381–2395. doi:10.1109/tsg.2019.2953716

Liu, J., Qin, C., and Yu, Y. (2019b). Enhancing distribution system resilience with proactive islanding and RCS-based fast fault isolation and service restoration. *IEEE Trans. Smart Grid* 11 (3), 2381–2395. doi:10.1109/tsg.2019.2953716

Mu, Y., Li, L., Hou, K., Meng, X., Jia, H., Yu, X., et al. (2022). A risk management framework for power distribution networks undergoing a typhoon disaster. *IET Generation, Transm. Distribution* 16 (2), 293–304. doi:10.1049/gtd2.12305

Perera, A. T. D., Nik, V. M., Chen, D., Scartezzini, J. L., and Hong, T. (2020). Quantifying the impacts of climate change and extreme climate events on energy systems. *Nat. Energy* 5 (2), 150–159. doi:10.1038/s41560-020-0558-0

Shi, Q., Li, F., Dong, J., Olama, M., Wang, X., Winstead, C., et al. (2022). Co-optimization of repairs and dynamic network reconfiguration for improved distribution system resilience. *Appl. Energy* 318, 119245. doi:10.1016/j.apenergy.2022.119245

Van Hentenryck, P., Coffrin, C., and Bent, R. (2011). "Vehicle routing for the last mile of power system restoration," in Proceedings of the 17th Power Systems Computation Conference (PSCC'11), Stockholm, Sweden, 22-26 August 2011.

Yao, S., Wang, P., Liu, X., Zhang, H., and Zhao, T. (2020). Rolling optimization of mobile energystorage fleets for resilient service restoration. *IEEE Trans. Smart Grid* 11 (2), 1030–1043. doi:10.1109/tsg.2019.2930012

Yao, S., Wang, P., and Zhao, T. (2019). Transportable energy storage for moreresilient distribution systems with multiple microgrids. *IEEE Trans. Smart Grid* 10 (3), 3331–3341. doi:10.1109/tsg.2018.2824820

Zhang, G., Zhang, F., Zhang, X., Meng, K., and Dong, Z. Y. (2020). Sequential disaster recovery model for distribution systems with Co-optimization of maintenance and restoration crew dispatch. *IEEE Trans. Smart Grid* 11 (6), 4700–4713. doi:10.1109/tsg.2020.2994111

Zhang, G., Zhong, H., Tan, Z., Cheng, T., Xia, Q., Kang, C., et al. (2022). Texas electric power crisis of 2021 warns of a new blackout mechanism. *CSEE J. Power Energy Syst.* 8 (1), 1–9. doi:10.17775/CSEEJPES.2021.07720